REST Journal on Emerging trends in Modelling and Manufacturing
Vol:4(1),2018
REST Publisher
ISSN: 2455-4537

Website: www.restpublisher.com/journals/jemm

Exploration of Schottky junction properties of silver metallised ZnO for the photocatalytic activity

G. Poornima and L. Gomathi Devi*
Department of Post Graduate Studies in Chemistry, Central College City Campus,
Dr. Ambedkar Street, Bangalore University, Bangalore 560001, India
E-mail: poornimag.hariprasad@gmail.com & gomatidevi_naik@yahoo.co.in

Abstract

ZnO photocatalyst was prepared by sol-gel method. Silver metallization on the surface of ZnO was carried out by photoreduction method by varying the silver content from 0.1 to 1.0 wt %. PXRD pattern shows typical hexagonal wurtzite structure for ZnO and Ag-ZnO samples. At higher concentrations of silver, peaks pertaining to metallic silver and silver oxide were observed in the PXRD pattern. UV-vis absorbance spectra shows higher absorbance for silver metallised samples with extended absorption in the visible region due to the surface plasmon resonance (SPR) effect due to the oscillation of CB electrons. The band gap values of various catalysts were found to be 3.19, 3.14, 3.13, and 3.17 eV for SG-ZnO, Ag-ZnO (0.1 wt %), Ag-ZnO (0.5 wt %) and Ag-ZnO (1.0 wt %) respectively. The decreasing order of reactivity of the catalysts is as follows: Ag-ZnO (0.5 wt %) > Ag-ZnO (1.0 wt %) > SG-ZnO > Ag-ZnO (0.1 wt %).

1. Introduction

Among the numerous semiconductor materials, ZnO is one of the excellent photocatalyst that has been extensively studied owing to its unique physical and chemical properties, such as variable morphologies, low cost, high reaction activity and nontoxicity. Many research studies have highlighted the better performance of ZnO particles to remove some of the organic contaminants in the ground water. ZnO is a wide band gap material and its band edge positions can be compared to the TiO_2 which is popularly used in the field of photocatalysis. But ZnO like TiO_2 absorbs only in the UV region and the photogenerated charge carrier recombination is the major limitation (*1*). To overcome these limitations metal nanoparticles are often deposited on the surface of ZnO nanoparticles. The metal nano deposits acts as trapping sites by accepting the photogenerated electrons from the conduction band of ZnO (*2-5*). Deposition of noble metals like Au, Ag and Pt nanoparticles effectively reduces the charge carrier recombination. The Fermi level of the semiconductor and the electron accepting states of surface deposited noble metal should match with one another (*6-8*). Recently, Xie et al. showed that depositing Ag on ZnO nanostructures improved photocatalytic activity due to stable separation of photogenerated electrons and holes (*9*). They demonstrated that only 80 min were taken to fully degrade methylene blue (MB) under UV light, using Ag/ZnO nanostructures. Liu et al. studied the effect of Ag-deposited ZnO nanostructures for degrading Rhodamine-B (RhB) and confirmed an enhancement in photocatalytic efficiency (*10*). Deng et al. decorated ZnO microrods with photoreduced Ag nanoparticles and the combined structures were found to increase the rate of degradation of MB under both UV and solar light compared to pure ZnO microrods (*11*). Although all of the aforementioned results have shown the enhanced photocatalytic activity, none of the research articles deal with the prevention of corrosion of ZnO nanoparticles especially in alkaline conditions and lacks the discussion pertaining to the exact mechanism of charge transfer process (*12, 13*). In this regard, Ag has been chosen to be deposited on ZnO, since it is less expensive compared to Au and Pt and has energy level below the conduction band (CB) of ZnO. Ag occupies exceptionally special position among the metals from the point of view of electronic properties. The work function of Ag ($\Phi \sim 4.7$ eV) is much lower than the work function of the other noble metals especially Au and Pt. Other exceptional properties of Ag are that it is resistant to dissolution, it can resist the attack of oxidizing agent and enhance the activity of ZnO.

2. Experimental

2.1 Materials

Zinc nitrate hexahydrate ($Zn(NO_3)_2 \cdot 6H_2O$) 99% purity, sodium hydroxide (NaOH) and sulphuric acid (H_2SO_4) were obtained from Merck Chemicals Limited. Silver nitrate was obtained from Sisco-Chemical Industries. Ammonia was obtained from SD Fine Chemicals and Rhodamine B (RhB) (dimethyl amino-azobenzene sodium sulphonate) was obtained from Aldrich Chemicals. All the reagents used were of analytical grade and the solutions were prepared using double distilled water.

2.2 Catalyst preparation

2.2.1 Preparation of ZnO photocatalyst

ZnO was prepared by sol–gel method as previously reported (*2, 14*). $Zn(NO_3)_2 \cdot 6H_2O$ was dissolved in distilled water to form an aqueous solution, 0.2 M ammonia (28 wt %) was then added drop wise to the aqueous solution with continuous stirring for 1 h. The white precipitate was filtered and the product was repeatedly washed with water to remove all nitrate ions and

further it was washed with ethanol and then dried in oven at 90 °C for 1 h and finally calcined at 450 °C for 5 h in a muffle furnace.

2.2.2 Process of surface Ag deposition on ZnO photocatalyst

Silver deposition on the surface of the photocatalyst was carried out by photoreduction of $AgNO_3$ in the presence of oxalic acid in an aqueous suspension as prepared by Szabo-Bardos et al. [*3, 15, 16*]. Silver concentration was varied from 0.1 to 1.0 wt % on the surface of the ZnO photocatalyst by varying the concentration of silver nitrate. An aqueous solution of $AgNO_3$ (1.24×10^{-4} M) and oxalic acid (5×10^{-3} M) along with ZnO (1 g) was suspended in 1 L of distilled water and was stirred vigorously under UV irradiation for 40–50 min to get 0.1 wt % of silver deposit. Silver deposited samples were designated as Ag-ZnO(X), where X is the Ag weight percentage and is equal to 0.1, 0.5 and 1.0 wt %. The pH of the suspension was adjusted to 6.8–7.0 by the addition of 0.1 N NaOH solution. After the irradiation, the solution containing Ag-ZnO(X) was allowed to stand for 6 h. Depending on the percentage of deposited silver the color of the photocatalyst changed from white to dark grey indicating the reduction of Ag^+ to Ag^0 and confirming the deposition of Ag^0 on the surface of ZnO. The solid was filtered, washed, dried and then heated at 120 °C for 2 h. The absence of silver in the aliquot sample of reaction mixture confirms the complete deposition of Ag metal on the semiconductor particle surface.

2.3 Characterization of the catalysts

The PXRD patterns of the catalysts were recorded using Panalytical X'Pert Pro MPD: PW3204 diffractometer at room temperature using Cu Kα radiation as source with Ni filter under the scan rate of 2° per min in the 2θ range of 20–80°. The absorption spectra were recorded by using a Shimadzu- UV 3101 PC UV-VIS-NIR UV–vis spectrophotometer in the range of 200–800 nm. The baseline correction was done using a calibrated sample of $BaSO_4$. FTIR spectra were obtained using Agilent Technologies Cary 630 FTIR spectrometer over the range of frequencies from 4,000–400 cm^{-1} using KBr as the reference sample. The morphology of the photocatalysts was observed using scanning electron microscope (SEM, JEOL JSM-6490LV). EDX technique was employed to obtain the information of the percentage of elements present in the samples.

2.4 Photochemical reactor and photocatalytic experiments

The photocatalytic activity of all the prepared samples were evaluated in the degradation of RhB under UV/solar light and the reaction conditions were optimized to achieve maximum efficiency within the desired interval time. Experiments were carried out at room temperature using a circular glass reactor whose surface area was 176.6 cm^2. Before the start of the reaction, the catalysts were finely dispersed in 250 ml of the dye solution and stirred in dark for 30 min to ensure adsorption equilibrium of the dye on the catalyst surface under the specific pH conditions. 125 W medium pressure mercury vapour lamp was used as the UV light source. Photon flux was found to be 7.8 m W/cm^2 by ferrioxalate actinometry whose wavelength peaks around 350-380 nm is used. The irradiation was carried out by direct focusing the light into the reaction mixture in open air condition at a distance of 29 cm. The reaction mixture was continuously stirred. Solar light experiments were performed under sunlight directly between 11 am to 2 pm when the solar intensity fluctuations were minimal. The intensity of sunlight was found to be around 1200 W/m 2. A convex lens was used for focusing and concentrating the solar light intensity and the reaction mixture was exposed to this concentrated sunlight. The average solar intensity was found to be 0.776 kW m^{-2} by solar radiometer. The intensity of the solar light was concentrated by using a convex lens and the reaction mixture was exposed to this concentrated sunlight. The solar radiation as a function of wavelength was measured by photometer, which shows the maximum around 450–500 nm. To avoid the error arising due to the fluctuations in solar intensity, all the experiments were conducted simultaneously.

A typical experiment contains 100 mg of catalyst finely dispersed in 250 ml of 10 ppm RhB dye solution under the specified conditions that was stirred vigorously using magnetic stirrer. The test samples were taken out at different time intervals and the solution was centrifuged at 1500 rpm for 2 minutes and then filtered to remove the catalyst particles completely. The RhB dye concentration in the aqueous phase was estimated using an UV–vis spectrophotometer. A blank experiment containing only the substrate RhB in the absence of photocatalyst with illumination was performed in order to determine the contribution of the direct photolysis.

3. Results and Discussion

3.1 PXRD studies

The PXRD patterns of SG-ZnO and Ag-ZnO(X) photocatalysts are displayed in Fig. 1. The diffraction peaks at 31.8^0, 34.4^0, 36.2^0, 47.5^0, 56.6^0, 62.8^0, 66.4^0, 67.9^0 and 69.1^0 were ascribed to (100), (002), (101), (102), (110), (103), (200), (112) and (201) planes of ZnO (JCPDS No.36-1451) confirming typical hexagonal wurtzite ZnO. The minor diffraction peaks at 38.18^0, 44^0 and 64^0 are ascribed to (111), (200) and (311) indicating the presence of metallic silver (JCPDS No. 04-0783) which is more prominently present in the 1.0 wt % Ag-ZnO sample.

The average crystallite size was estimated based on the broadening of (101) peak at $2\theta = 36.2^0$ using the Scherrer's equation $d = \frac{k\lambda}{\beta \cos\theta}$, where λ is the wavelength of the Cu Kα source used, β is the full width at half maximum (FWHM) of the (101) diffraction angle, *k* is a shape factor (0.94) and θ is the angle of diffraction. There is no change in the diffraction peaks of Ag deposited ZnO. With an increase of Ag content, the diffraction peak of Ag (111) becomes much stronger and sharper which indicates the increase in the mean size of metal Ag particles.

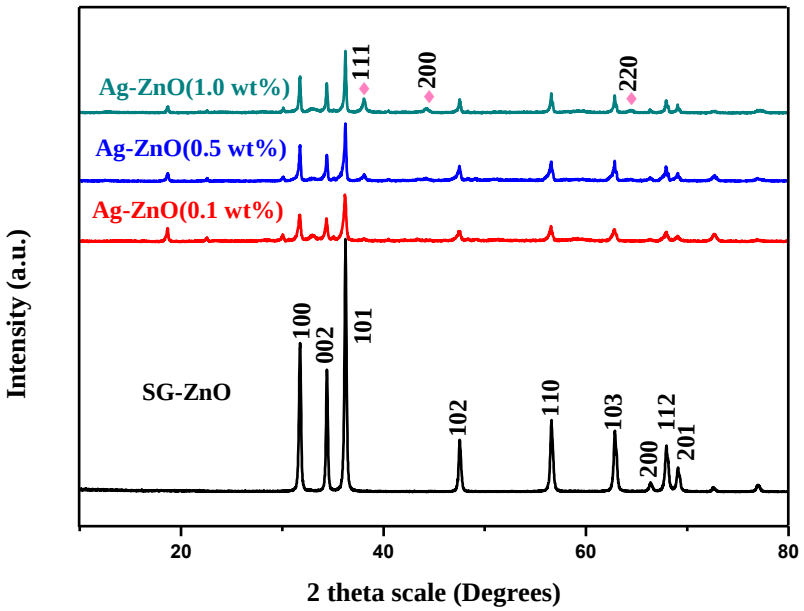

Fig 1. PXRD pattern of the Sg-ZnO, Ag-ZnO (0.1 wt %), Ag-ZnO (0.5 wt %) and Ag-ZnO (1.0 wt %) samples

Photocatalysts	Crystallite size D (nm)	Lattice parameters (Å)	Unit cell volume $(Å)^3$	λ_{max} (nm)	E_g (eV)
SG-ZnO	34.9016	a=b=2.8163; c=5.412	42.925	389.176	3.2
Ag-ZnO (0.1 wt %)	29.3272	a=b=2.8225; c=5.219	41.577	390.399	3.16
Ag-ZnO (0.5 wt %)	40.0654	a=b=2.8168; c=5.212	41.353	396.792	3.13
Ag-ZnO (1.0 wt %)	44.3746	a=b=2.8167; c=5.211	41.350	395.194	3.18

Table 1. Summary of data obtained by X-ray diffraction and UV–vis absorption techniques. D: crystallite size in nm, Å: lattice parameters, $(Å)^3$: unit cell volume, λ_{max}: absorption maxima in nm, and E_g: band gap energies in eV.

3.2 UV-visible absorbance spectral studies

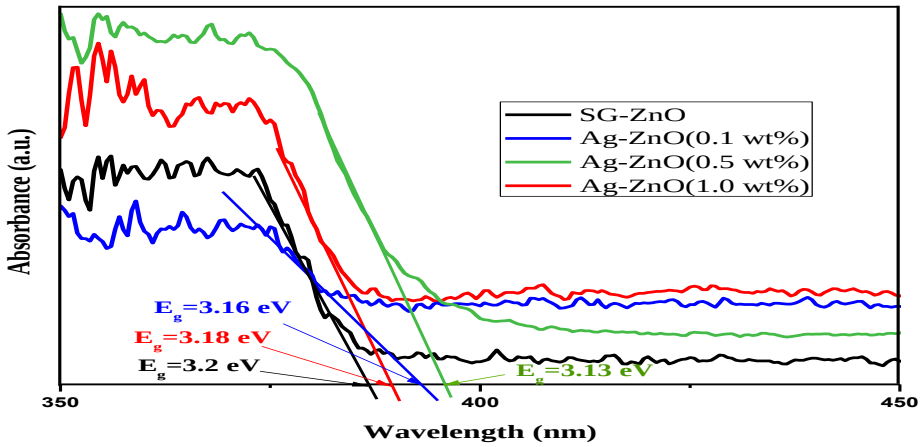

Fig. 2. UV-vis absorption spectra of SG-ZnO and Ag-ZnO(X) samples

The optical absorption properties of catalysts were investigated using UV-visible absorption spectral technique. Fig. 2 shows the UV–vis absorbance spectra of SG-ZnO and Ag-ZnO(X) photocatalysts. Modification of ZnO with Ag remarkably influenced the optical properties of the photocatalysts. It was observed that the Ag-ZnO samples exhibited improved optical response in the visible region after the surface deposition of metallic Ag^0. The intensity of the reflected radiation provides information about the wavelength at which the semiconductor absorbs the light. The absorption spectra of the deposited

samples shows extended absorption in the higher wavelength region. The extent of absorption of Ag-ZnO (0.5 wt %) was found to be maximum under UV region and an extended absorption is also maximum in the visible region. Further, increase in the Ag concentration the extent of absorption decreases for Ag-ZnO (1.0 wt %) sample implying the optimum concentration to be 0.5 wt % of Ag on ZnO surface. The band gap energy values of the samples can be calculated using the equation: $E_g = \frac{1240}{\lambda}$; where, E_g is the band gap energy (eV) and the value of λ (nm) is obtained from the intersection point of tangents drawn to the absorption curves on the wavelength axis.

3.3 SEM and EDX

In order to investigate the morphology of the synthesized photocatalyst particles, SEM and EDX analysis were carried out. Fig. S1 shows SEM images of SG-ZnO (Fig. S1A), Ag-ZnO (0.1 wt %) (Fig. S1B), Ag-ZnO (0.5 wt %) (Fig. S1C) and Ag-ZnO (1.0 wt %) (Fig. S1D) photocatalysts. The SEM images show that the silver particles are homogeneously distributed on the surface of ZnO photocatalyst. The Fig. S1B shows the hexagonal morphology of ZnO, but as the concentration of silver content increases, it covers up the hexagonal morphology of ZnO photocatalyst. EDX spectra of Ag-ZnO (1.0 wt %) is shown in Fig. S1E. The presence of Ag, Zn and O were confirmed in the Ag-ZnO (0.5 wt %) and Ag-ZnO (1.0 wt %) samples. Qualitative and quantitative determination of elements present in the sample was done by using grid supported carbon film of 15–25 nm thickness which gives exceptionally low background. The atomic % and weight % values of elements in various samples are given in Table S2. The fractional percentage of carbon detected was neglected in this study since the grid supported carbon film was used.

3.4 FTIR analysis

FTIR spectrum for ZnO shows two bands around 350–600 cm^{-1}, which are generally assigned to the stretching vibration of Zn–O bond (Fig. 3). The bands at 3372 cm^{-1} and 1597 cm^{-1} corresponds to the O-H stretching and O-H bending vibrations of the surface adsorbed water molecule. The spectra of the Ag-ZnO(X) samples display well-defined characteristic bonds which are not seen for the SG-ZnO sample. The band at 3393 cm^{-1} corresponds to the stretching vibrations of –OH groups of ZnO is narrowed and shifted to a lower frequency of 3360 cm^{-1} for Ag-ZnO(X) samples. Such characteristic shifts can be attributed to the hydrogen bonding. The appearance of three sharp peaks at 1620 cm^{-1}, 1494 cm^{-1} and 1345 cm^{-1} is due to the bond formation between silver and oxygen.

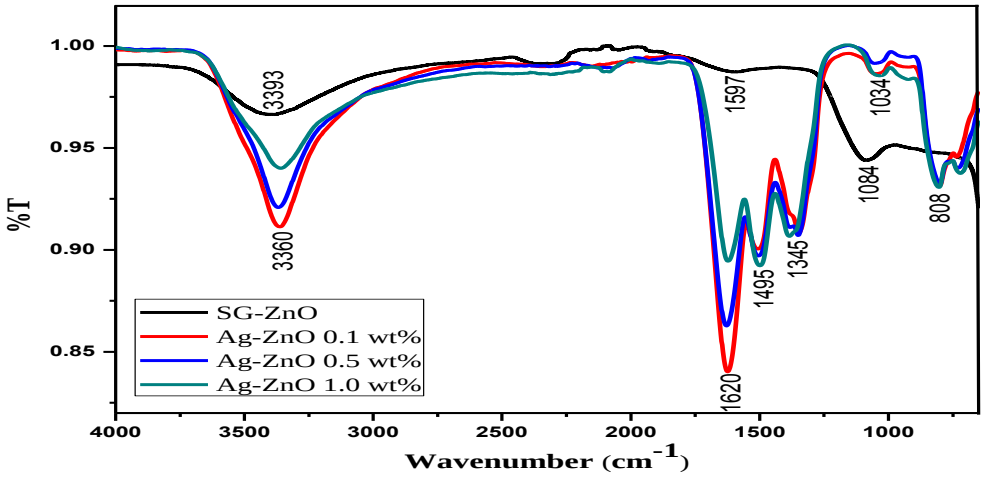

Fig 3. FTIR spectra of SG-ZnO and Ag-ZnO(X) samples

3.5 Photocatalytic activity

The photocatalytic activity of the SG-ZnO and Ag-ZnO(X) was studied by taking RhB as a model pollutant under UV and visible light irradiation. Fig 4 shows the plots of C/C_0 versus time for the degradation of RhB in the presence of different catalysts (Ag-ZnO(X) and SG-ZnO) under UV/visible light illumination, where C is the concentration of RhB remaining in the solution after irradiation time t and C_0 is the initial concentration of the RhB. The blank experiments reveal 40% of degradation of RhB which is direct photolysis process. The decreasing order of reactivity of the catalysts under UV and solar light irradiation is as follows: Ag-ZnO (0.5 wt %) > Ag-ZnO (1.0 wt %) > SG-ZnO > Ag-ZnO (0.1 wt %). Ag-ZnO (0.5 wt %) catalyst shows highest efficiency. Ag-ZnO (0.5 wt %) photocatalyst shows 100% degradation within 30 minutes. The surface deposited silver particles at optimum concentration traps the photoinduced electrons and later these electrons are detrapped to the adsorbed oxygen molecule to form $O_2^{\bullet-}$ radical. The electron-hole separation is enhanced which contributes to enhanced photocatalytic activity during the interfacial charge transfer process at the interface of the Ag and ZnO contact.

This creates the Schottky barrier due to the differences in the work function of Ag and ZnO. This barrier mainly traps the electrons thereby reducing the rate of recombination of electron-hole pairs.

$$ZnO + h\upsilon \rightarrow ZnO(e^-_{CB} + h^+_{VB}) \quad (1)$$

$$e^-_{CB} + O_2 \rightarrow O_2^{\bullet -} \quad (2)$$

$$h^+_{VB} + OH \rightarrow {}^{\bullet}OH \quad (3)$$

$${}^{\bullet}OH + RhB \rightarrow \text{degradation product} \quad (4)$$

Under solar light, ZnO showed no visible light absorption. The irradiated visible light is absorbed mainly by RhB and also by Ag^0 by surface plasmon resonance effect (*17*). Upon the absorption of light by RhB, an electron is excited to higher energy levels and further transferred to the CB of ZnO. This mechanism is called a dye-sensitization (*18*). The transfer rate is determined by the interfacial wave-function of the catalyst and the dye (*19-21*). The CB electron is then captured by the adsorbed oxygen to form an active $O_2^{\bullet -}$ species (*19-23*). The photogenerated superoxide radicals degrade the RhB. The holes (h^+_{VB}) react with OH^- or H_2O to form active ${}^{\bullet}OH$ radicals.

$$Ag + \text{Visible light} \rightarrow Ag^* \quad (5)$$

$$Ag^* + ZnO \rightarrow Ag + ZnO(e^-_{CB}) \quad (6)$$

$$RhB + \text{Visible light} \rightarrow RhB^*(e^-_{CB} + h^+_{VB}) \quad (7)$$

$$RhB^*(e^-_{CB} + h^+_{VB}) + ZnO \rightarrow ZnO(e^-_{CB}) + RhB\,(h^+_{VB}) \quad (8)$$

$$ZnO(e^-_{CB}) + \text{adsorbed } O_2 \rightarrow O_2^{\bullet -} + ZnO \quad (9)$$

$$O_2^{\bullet -} + H^+ \rightarrow {}^{\bullet}OH \quad (10)$$

$$H_2O + ZnO(h^+_{VB}) \rightarrow H^+ + {}^{\bullet}OH \quad (11)$$

$$OH^- + ZnO(h^+_{VB}) \rightarrow {}^{\bullet}OH \quad (12)$$

$$\text{Active } O_2^{\bullet -}, H^+ \text{ or } {}^{\bullet}OH \text{ species} + \text{adsorbed RhB dye} \rightarrow \text{degradation products} \quad (13)$$

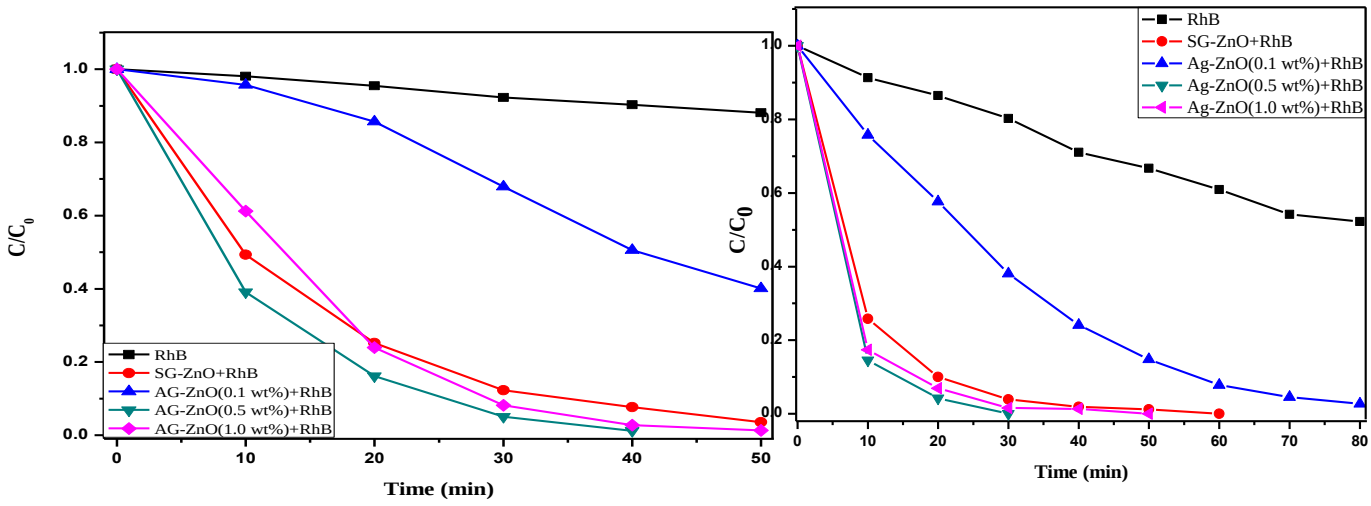

Fig. 4. Plots of C/C_0 versus time for degradation of RhB under: **(A)** UV light irradiation and **(B)** Solar light irradiation.

The energy level of the deposited Ag varies with its size and plays a crucial role in interfacial electron transfer process in the photocatalysis. The energy level of the single Ag atom is around -1.30 eV and for the bulky Ag deposits it is around -4.6 eV versus vacuum energy level. The energy level of the $O_2/O_2^{\bullet -}$ is found to be around -4.27 eV versus vacuum energy level. As the size of the Ag atoms increases its energy levels are lowered and are located below the CB of ZnO. The main criteria for the photoinduced interfacial electron transfer depends on the energy level of the CB of ZnO and the deposited silver atoms (varies from -4.64 eV to -1.30 eV versus vacuum energy level) and dissolved oxygen molecules (-4.27 eV versus vacuum energy level) as shown in the Fig. 5. The energy level of the single Ag atom lies above the CB edge of ZnO and the electrons cannot migrate to this Ag atom, since electrons cannot move uphill. Hence the Ag-ZnO (0.1 wt %) sample shows lower photocatalytic activity compared to the other samples. The energy level of the bulky silver atoms can be found below the CB

of ZnO, but if the energy level of the dissolved oxygen molecule is above, the electrons cannot migrate to the molecular oxygen. These mechanisms are depicted elaborately in the Fig. 5. At optimum Ag deposition (0.5 wt %), the Ag energy level is below the CB of ZnO and it is above the energy level of dissolved oxygen molecule (-4.27 eV versus vacuum energy level). Hence the photoinduced electrons can migrate smoothly from the CB of ZnO to the deposited Ag atoms and in turn can migrate to the oxygen molecule, this speed up the interfacial charge transfer process.

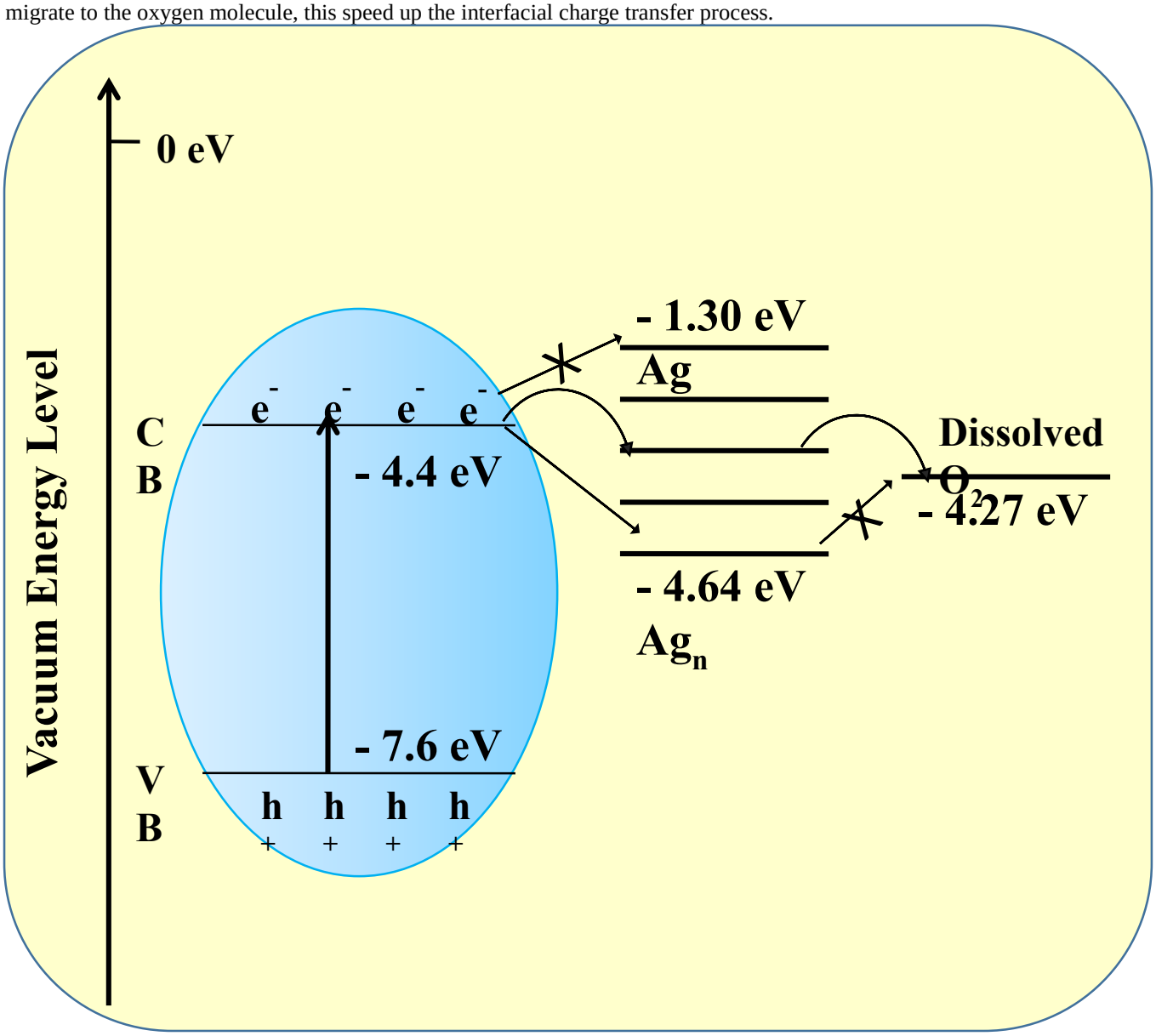

Fig. 5. The energy level diagram of ZnO, Ag deposit and dissolved oxygen depicting the overall charge transfer mechanism.

4. Conclusion

The surface modification of ZnO with metallic silver is one of the methods proposed in the present research to enhance the photocatalytic activity by reducing the rate of recombination of photogenerated charge carriers. The enhanced activity of silver metallised ZnO under solar light can be attributed to the surface plasmon resonance effect of Ag nanoparticles which creates an enhanced local electric field on the surface of ZnO. The plasmon resonance energy depends on size, shape and concentration of the metal nano deposits.

Acknowledgement

Authors acknowledge the financial assistance from University Grants Commission (UGC) for Rajeev Gandhi National Fellowship and Department of Science and Technology (DST).

Conflict of Interest

There are no conflicts of interest.

References

[1]. Zengxia Pei, Luyao Ding, Meiliang Lu, Zihan Fan, Sunxian Weng, Jun Hu, and Ping Liu. "Synergistic effect in polyanaline-hybrid defective ZnO with enhanced photocatalytic activity and stability." *The Journal of Physical Chemistry C* 118 (2014):9570-9577.

[2]. L. Gomathi Devi, M.L. Aruna Kumari, B.G. Anitha, R. Shyamala, and G. Poornima. "Photocatalytic evaluation of Hemin (chloro(protoporhyinato)iron(III)) anchored ZnO hetero-aggregate system under UV/solar light irradiation: A surface modification method." Surfaces and Interfaces 1–3 (2016): 52–58.
[3]. B. Nagaraj, L. Gomathi Devi. "Silver metalized mixed phase manganese-doped titania: Variation ofelectric field and band bending within the space charge region with respect to the silver content." *Journal of Molecular Catalysis A: Chemical* 390 (2014): 142–151.
[4]. J. M. Hermann, H. Tahiri, Y. Ait-Ichou, G. Lossaletta, A.R. Gonzalez-Elipe, A. Fernandez. "Characterization and photocatalytic activity in aqueous medium of TiO_2 and Ag-TiO_2 coating on quartz." *Applied Catalysis B: Environmental* 13 (1997): 219-228.
[5]. Prashant V. Kamat. "Photophysical, photochemical and photocatalytic aspects of metal nanoparticles." *Journal of Physical Chemistry B* 106 (2002): 7729.
[6]. Elias Stathatos, Tatyana Petrova, Panagiotis Lianos. "Study of efficiency of visible-light photocatalytic degradation of basic blue adsorbed on pure and doped mesoporous titania films." *Langmuir* 17 (2001): 5025-5030
[7]. Ronghua Wang, John Haozhong Xin, Yang Yang, Hongfang Liu, Liming Xu, Junhui Hu. "The characteristics and photocatalytic activity of silver doped ZnO nanocrystallites." *Journal of Applied Surface Science*, 227 (1-4) (2004): 312-317.
[8]. Reenamole Georgekutty, Michael K. Seery, and Suresh C. Pillai. "A Highly Efficient Ag-ZnO Photocatalyst: Synthesis, Properties, and Mechanism." *Journal of Physical Chemistry C* 112 (2008): 13563–13570.
[9]. W. Xie, Y. Li, W. Sun, J. Huang, H. Xie, X. Zhao. "Surface modification of ZnO with
[10]. Ag improves its photocatalytic efficiency and photostability." *Journal of Photochemistry and Photobiology A* 216 (2) (2010): 149–155.
[11]. H. Liu, G. Shao, J. Zhao, Z. Zhang, Y. Zhang, J. Liang, X. Liu, H. Jia, B. Xu. "Wormlike Ag/ZnO core-shell heterostructural composites: fabrication, characterization, and photocatalysis." *Journal of Physical Chemistry C* 116 (30) (2012): 16182–16190.
[12]. Q. Deng, X. Duan, D.H. Nguyen, H. Tang, Y. Yang, M. Kong, Z. Wu, W. Cai, G. Wang. "Ag nanoparticle decorated nanoporous ZnO microrods and their enhanced photocatalytic activities." *ACS Applied Material and Interfaces* 4 (11) (2012): 6030–6037.
[13]. X. Li, F. Li. "Study of Au/Au^{3+}-TiO_2 photocatalysts toward visible photooxidation for water and wastewater treatment." *Environmental Science and Technology* 35 (11) (2001): 2381–2387.
[14]. J. Yu, L. Yue, S. Liu, B. Huang, X. Zhang. "Hydrothermal preparation and photocatalytic activity of mesoporous Au-TiO_2 nanocomposite microspheres." *Journal of Colloid Interface Science* 334 (1) (2009): 58–64.
[15]. Dong En Zhang, Jun Yan Gong, Juan Juan Ma, Gui Quan Han and Zhi Wei Tong. "A facile method for synthesis of N-doped ZnO mesoporous nanospheres and enhanced photocatalytic activity." *Dalton Transactions* 42 (2013): 16556–16561.
[16]. L. Gomathi Devi, B.Nagaraj. and K. Eraiah Rajashekhar. "Synergistic effect of Ag deposition and nitrogen doping in TiO_2 for the degradation of phenol under solar irradiation in presence of electron acceptor." *Chemical Engineering. Journal*. 181-182 (2012): 259–266.
[17]. Erzsébet Szabó-Bárdos, Hajnalka Czili, Attila Horváth. "Photocatalytic oxidation of oxalic acid enhanced by silver deposition on a TiO_2 surface." *Journal of Photochemistry and Photobiology A: Chemistry* 154 (2003): 195–201.
[18]. Y. Zang, J. Yin, X. He, C. Yue, Z. Wu, J. Li and J. Kang. "Plasmonic-enhanced selfcleaning activity on asymmetric Ag/ZnO surface-enhanced Raman scattering substrates
[19]. under UV and visible light irradiation." *Journal of Material Chemistry A* 2 (2014): 7747-7753.
[20]. B. Subash, B. Krishnakumar, M. Swaminathan and M. Shanthi. "Highly Efficient, Solar Active, and Reusable Photocatalyst: Zr-Loaded Ag−ZnO for Reactive Red 120 Dye Degradation with Synergistic Effect and Dye-Sensitized Mechanism." *Langmuir* 29 (2013): 939−949.
[21]. W. Kim, D. Pradhan, B. Min and Y. Sohn. "Adsorption/photocatalytic activity and fundamental natures of BiOCl and $BiOCl_xI_{1-x}$ prepared in water and ethylene glycol environments, and Ag and Au-doping effects." *Applied Catalysis B* 147 (2014): 711-725.
[22]. Y. Park, Y. Na, D. Pradhan, B. Min and Y. Sohn. "Adsorption and UV/Visible photocatalytic performance of BiOI for methyl orange, Rhodamine B and methylene blue: Ag and Ti-loading effects." *CrystEngComm* 16 (2014): 3155–3167.
[23]. Y. Na, Y. Kim, D. Cho, D. Pradhan and Y. Sohn. "Adsorption/photocatalytic performances of hierarchical flowerlike $BiOBr_xCl_{1-x}$ nanostructures for methyl orange, Rhodamine B and methylene blue." *Material Science in Semiconductor Processing* 27 (2014): 181-190.
[24]. A. Nayak, S. Lee, Y. Sohn, D. Pradhan. "Synthesis of In2S3 microspheres using a template-free and surfactant-less hydrothermal process and their visible light photocatalysis." *CrystEngComm* 16 (2014): 8064-8072.
[25]. Young In Choi, Hye Jin Jung, Weon Gyu Shin, and Youngku Sohn. "Band gap-engineered ZnO and Ag/ZnO by ball-milling method and their photocatalytic and Fenton-like photocatalytic activities." *Applied Surface Science* 356 (2015): 615-625.

Electronic Supplementary Material
SEM and EDX

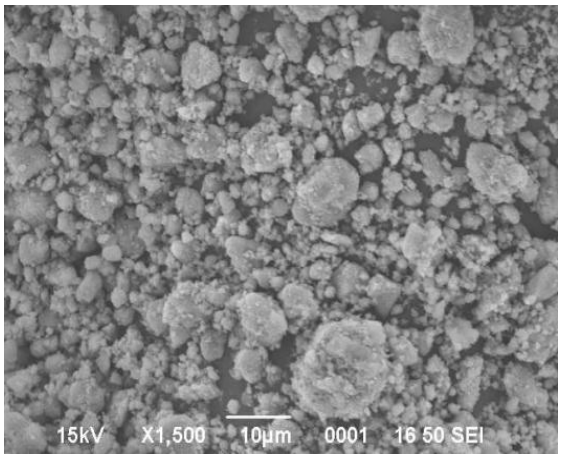

Fig. S1(A)

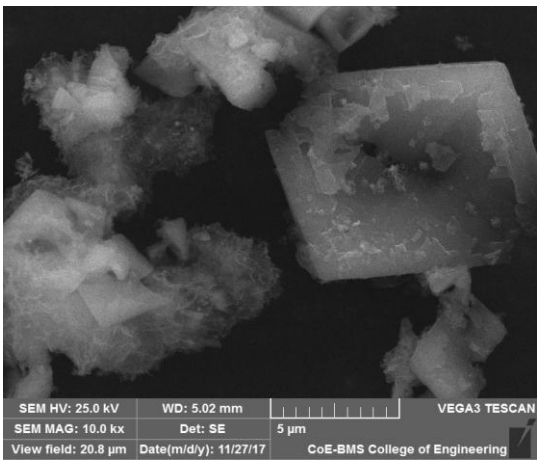

Fig. S1(B)

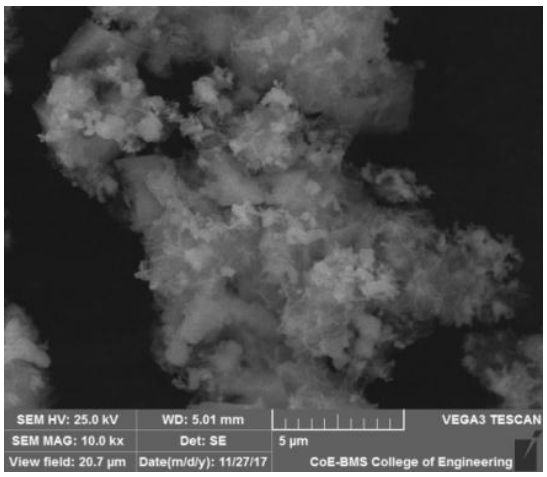

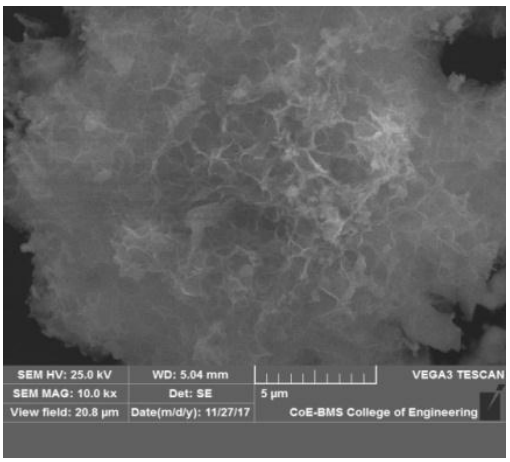

Fig. S1(C) **Fig. S1(D)**

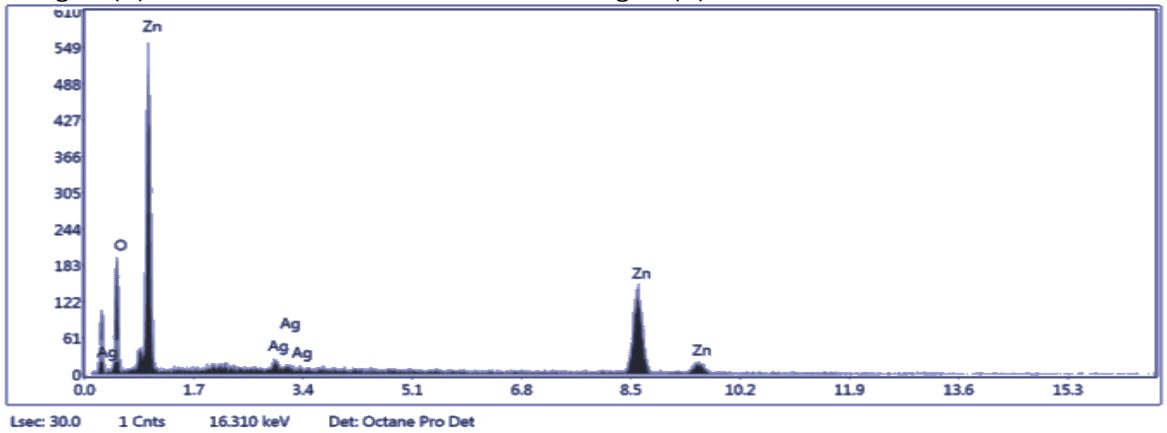

Fig. S1(E)

Fig.S1. SEM images of (A) SG-ZnO (B) Ag-ZnO (0.1 wt %) showing hexagonal wurtzite structure (C) Ag-ZnO (0.5 wt %) (D) Ag-ZnO (1.0 wt %) and (E) EDX pattern of Ag-ZnO (1.0 wt %)

Photocatalyst	Element	Weight%		Atom%	
		Observed	Approximate	Observed	Approximate
SG-ZnO	Zn	53.04	53	24.36	24
	O	46.87	47	75.64	76
Ag-ZnO (0.1 wt %)	Ag	0.27	0.3	0.07	0.1
	Zn	56.10	56	23.92	24
	O	43.63	44	76.01	76
Ag-ZnO (0.5 wt %)	Ag	1.63	1.6	0.46	0.5
	Zn	61.72	62	29.05	29
	O	36.65	37	70.48	70
Ag-ZnO (1.0 wt %)	Ag	4.09	4	1.09	1
	Zn	53.97	54	23.69	24
	O	41.93	42	75.22	75

Table S2. EDX data of SG-ZnO, Ag-ZnO (0.1 wt %), Ag-ZnO (0.5 wt %) and Ag-ZnO (1.0 wt %).